Title: Determination of the volume fraction of precipitates in a nitrided Fe-0.354wt.%C-2.93wt.%Cr model alloy by anomalous small angle X-ray scattering

Authors: S. Jégou[a], M. Dumont[b,*], L. Barrallier[a]

[a] Arts et Métiers ParisTech, MSMP laboratory, 2 cours des Arts et Métiers, F-13617 Aix-en-Provence, France
[b] Aix Marseille Univ, Univ Toulon, CNRS, IM2NP, Marseille, France

*corresponding author: Dr. Myriam Dumont

Phone: +33 4 91 28 90 09

Fax: +33 4 91 28 28 86

e-mail: myriam.dumont@univ-amu.fr

Postal address:

Myriam Dumont

IM2NP – UMR CNRS 7334 – Aix-Marseille Université

Faculté des Sciences et Techniques de St-Jérôme – Service 251

13 397 Marseille Cedex 20

France

Abstract:

Anomalous small angle scattering (ASAXS) is a powerful non-destructive technique that can provide characteristic features of nanoscale precipitates such as the volume fraction, and chemical composition. In this paper, the technique is used for the first time to explore nanoscale MN nitrides (M = Cr,Fe) after nitriding of a model iron alloy (Fe-0.354wt.%C-2.93wt.%Cr).

Keywords:

Steel; Nitriding; Nitrides; Synchrotron radiation; Anomalous small angle scattering.

1. Introduction

Anomalous small-angle X-ray scattering (ASAXS) is a powerful technique that combines the capability of SAXS to characterize the size distribution of nano-objects embedded in a matrix and the variation in contrast allowed by tunable wavelength of the Synchrotron incident X-ray beam, giving access to information about the composition of scattering nano-objects [1-2] .

In this study, ASAXS technique is applied to characterize precipitates in a ternary Fe-Cr-C nitrided steel. Nitriding is a surface engineering process applied to enhance surface properties such as corrosion, wear and fatigue resistance [3-4]. Gaseous nitriding consists in the diffusion of nitrogen atoms through the surface of steels from the dissociation of a nitrogen rich atmosphere (gas or plasma) at the atmosphere/solid interface [5]. It results in the formation of an iron nitride layer (Fe_4N and/or $Fe_{2-3}N$) and a diffusion zone where nitrogen is found as solid solution in the ferritic matrix and combined as MeN (Me = Cr, V, Al…) nitrides with alloying elements having high affinity with nitrogen such as chromium, aluminium or vanadium [6]. The volume fraction of ~~MN~~ nitrides formed in the diffusion

layer is of prime importance for requested surface properties. In fact this affects the resulting hardness; moreover the volume change induced by precipitation takes part to the generation of compressive residual stresses [7].

In the case of binary Fe-Me (Me=Cr, Al or V) alloy, formed nitrides are close to pure MeN phase having a fcc NaCl-type structure [5]. In the case of C-containing ternary Fe-Cr-C, pre-existing carbides (generally $M_{23}C_6$ or M_7C_3, M=Fe or Cr) are expected to dissolve due to a lower stability as compared to nitrides [8]. Therefore nitrides are formed either by direct formation by reaction with Cr remaining in solid solution or by transformation of carbides [9]. Carbon is then rejected toward grain boundaries where it forms coarse cementite aggregates [10] or towards the diffusion front where it participates to the coarsening of carbides.

This paper aims at using small-angle scattering to characterize ~~MN~~ nitrides in the diffusion layer after gas nitriding of a model ternary Fe-Cr-C alloy (Fe-0.354wt.%C-2.93wt.%Cr). The major goal is the determination of the volume fraction of nitrides that is the key parameter for resulting surface properties. However the volume fraction cannot be determined by SAXS independently of the composition of the nano-precipitates. Using anomalous dispersion effect, ASAXS is an element-selective technique based on the anomalous variation of the scattering factor near the absorption edge of one chosen element, therefore it allows to overcome this difficulty by giving access to the chemical information, allowing the determination of the volume fraction of scattering precipitates [11]. Results are discussed with respect to the literature and thermodynamics calculations performed using the Thermo-Calc software [12].

2. Materials and experimental methods

2.1. Materials and microstructural characterization

A Fe-0.354wt.%C-2.93wt.%Cr ternary alloy was used in this study. It was oil quenched and annealed at 590 °C. Gas nitriding was performed by Aubert & Duval at 550 °C during 100 h for a given nitrogen potential (K_N = 2.65 $atm^{-1/2}$). Composition profiles along the nitride layer were carried out by electron probe microanalysis (EPMA) as well as glow discharge optical emission spectrometry (GDOES) [7]. Observations of the case and core microstructure were carried out by optical microscopy as well as scanning and transmission electron microscopy.

2.2. Anomalous small angle scattering (ASAXS)

Small-Angle X-ray Scattering (SAXS) experiments were carried out on the BM02-D2AM, a French CRG beamline at the European Synchrotron Radiation Facilities (ESRF) in Grenoble. Regarding the composition of the system, the most reliable conditions for anomalous measurements are based on the Cr K-absorption edge. Four energies slightly below the Cr K-edge (5.96 keV) as well as one far from the Cr-edge were used for anomalous SAXS measurements. As SAXS experiments are performed in transmission mode, the relatively low energy of the Cr K-edge represented a challenge in the sample preparation since it required the preparation of relatively thin samples, around 30 μm in thickness, to ensure a satisfactory transmission through the thickness of the sample. Moreover in order to investigate the precipitation variations with depth (down to 1 mm), samples were cut along a bevel so that all depths can be studied by a profile measurement adapted to the lateral resolution of the beam (~300 μm). A preparation procedure was optimised and consisted in gently polishing 20×10 mm^2 surfaces using a bevel of ~3 degrees, so that 500 μm steps for profile measurement along samples correspond to 25 μm steps within the depth of the nitrided layer.

A small-angle set-up was chosen to well characterise nano-precipitates in the 2-50 nm radius range, i.e. in a q-range ranging from 0.03 nm^{-1} to 0.6 nm^{-1}, where q is the amplitude of the scattering vector q ($q = \frac{4\pi sin\theta}{\lambda}$ where θ is the half scattering angle and λ the wavelength). The SAXS patterns were acquired using a two-dimensional CCD camera. Data files were corrected from electronic noise, spatial distortion, pixel efficiency, the flat field of the detector, and background noise. A circular average was taken around the transmitted beam to obtain the intensity as a function of the scattering vector. The scattered intensity was finally converted into absolute values, I, using measurement of the intensity of the direct beam through calibrated filters.

The analysis method of ASAXS data to extract chemical information of nanoparticles is described in details in [11] and is summarised hereafter. The measured quantity used for the ASAXS analysis is the integrated intensity Q_0 defined as:

$$Q_0(\lambda) = \int_0^\infty I(q) q^2 dq = 2\pi^2 |\Delta\rho(\lambda)|^2 f_v(1 - f_v) \qquad \text{equation (1)}$$

where λ is the wavelength, q is the module of the scattering vector, f_v is the volume fraction of scattering objects, $\Delta\rho(\lambda)$ is the electronic contrast, defined as the difference in electronic density between the scattering particle (ρ_{ppt}) and the matrix (ρ_m) in which it is embedded: $|\Delta\rho| = |\rho_{ppt} - \rho_m|$.

The electronic contrast can be varied by changing the energy in a range close to the absorption edge of one element of the system. In fact, the electronic density of a phase constituted by N elements can be written:

$$\rho(\lambda) = \frac{\sum_{i=1}^{N} X_i f_i(\lambda)}{V_{at}} \qquad \text{equation (2)}$$

where X_i in the atomic fraction of element *i* $\left(\sum_{i=1}^{N} X_i = 1\right)$, V_{at} is the mean atomic volume of the particle or the matrix, $f_i(\lambda)$ is the atomic scattering factor of element *i*, which is tabulated as a function of the wavelength of the beam.

In the vicinity of the absorption edge of the element *k*, the electronic contrast can be written:

$$\left|\rho_{ppt} - \rho_m\right| = \frac{1}{V_{at,m}} \left| \sum_{\substack{i=1 \\ i \neq k}}^{N} \left[f_i \left(\alpha X_{i,ppt} - X_{i,m} \right) \right] + f_k(\lambda) \left(\alpha X_{k,ppt} - X_{k,m} \right) \right| \qquad \text{equation (3)}$$

with $\alpha = \frac{V_{at,m}}{V_{at,ppt}}$.

Using this formalism, $\sqrt{Q_0}$ is expected to vary linearly with the scattering factor $f_k(\lambda)$:

$$\sqrt{Q_o} = \theta + p f_k(\lambda) \qquad \text{equation (4)}$$

where :

$$\theta = \frac{\pi}{V_{at,m}} \sqrt{2 f_v (1 - f_v)}\, \delta \left(\sum_{\substack{i=1 \\ i \neq k}}^{N} f_i \left(\alpha X_{i,ppt} - X_{i,m} \right) \right)$$

$$p = \frac{\pi}{V_{at,m}} \sqrt{2 f_v (1 - f_v)}\, \delta \left(\alpha X_{k,ppt} - X_{k,m} \right)$$

with $\delta = 1$ if $\left(\rho_{ppt} - \rho_m\right) \geq 0$
$\delta = -1$ if $\left(\rho_{ppt} - \rho_m\right) < 0$.

Using the ratio θ / p is a straightforward way for extracting chemical information from ASAXS measurements (independently of the volume fraction):

$$\frac{\theta}{p} = \frac{\sum_{\substack{i=1 \\ i \neq k}}^{N} f_i \left(\alpha X_{i,ppt} - X_{i,m} \right)}{\left(\alpha X_{k,ppt} - X_{k,m} \right)} \qquad \text{equation (5)}$$

In the following, this approach is used to extract the Cr, Fe or N contribution to nitrides or matrix. In a second part the volume fraction of nitrides can be calculated using equation (1).

3. Results and discussion

3.1. Microstructure of the nitrided layer

Figure 1 gives in-depth composition profiles of carbon and nitrogen from the Fe-0.354wt.%C-2.93wt.%Cr alloy nitrided 100 h at 550 °C [7].

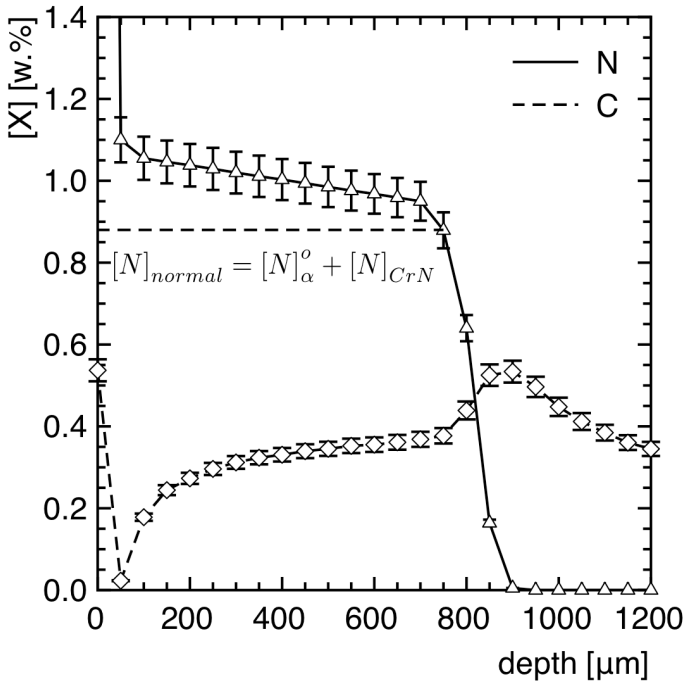

Figure 1: Nitrogen and carbon in-depth profiles of the Fe-0.354wt.%C-2.93wt.%Cr ternary alloy nitrided at 550 °C for 100 h (EPMA/GDOES analyses) [7]. “Normal” N content refers to the precipitation of all Cr atoms as binary CrN and the equilibrium solubility of nitrogen in the ferritic matrix ($[N]^{\circ}_{\alpha}$ = 0,05 wt.%) .

The diffusion layer stretches from 30 to 900 µm. The nitrogen in-depth profile is characterized by a smooth decrease from 1.2 (at 30 µm depth) to 0.95 wt.% (at 700 µm

depth) and a drop to the core content (0 wt.%) at a 900 µm depth. By defining a nitrogen limit, called "normal N content" in figure 1, which corresponds to the amount obtained by nitrogen fully reacting with chromium as CrN binary nitrides (considering the extremely low solubility of Cr in ferrite) added to the solubility limit of nitrogen in ferrite ($[N]°_{\alpha}$ = 0,05 wt.%), a nitrogen enrichment is observed through the diffusion layer. This so-called excess nitrogen, already observed in various systems, might be attributed to the substitution of alloying element in MN nitrides, or to an increase of the nitrogen solubility in the surrounding of MN nitrides due to local tensile straining accompanying their precipitation or by nitrogen adsorption at the precipitate/matrix interface. The carbon content profile shows a depletion of carbon close to the nitrogen rich region of the diffusion layer (at 50 µm depth) and an enrichment of carbon in front of the nitrogen diffusion front (at 900 µm depth). The diffusion of carbon backward to the surface or toward the core material during nitriding is ascribed to the transformation of initial carbides (M_7C_3, M = Cr or Fe) into alloying elements nitrides and cementite at grain boundaries [8,13].

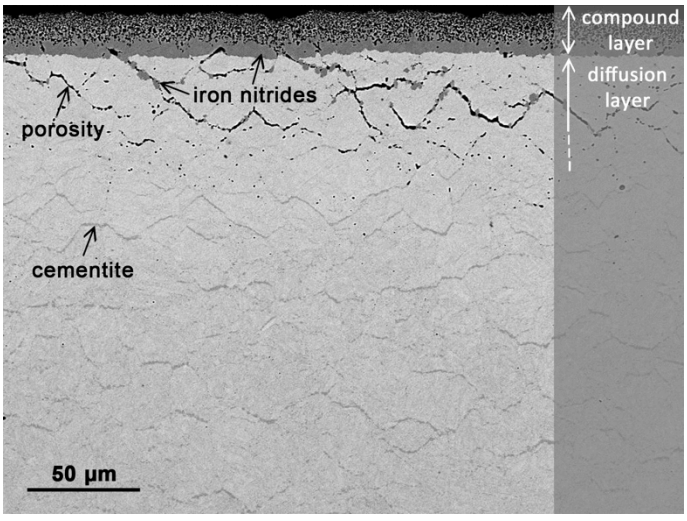

Figure 2: SEM micrograph (back scattering electron mode) from the case of a Fe-0.354wt.%C-2.93wt.%Cr ternary alloy nitrided at 550 °C for 100 h [14].

169 The microstructure of the first 250 μm of the case is given on Figure 2. It is characterized
170 by a compound layer of nearly 25 μm composed of iron nitrides $Fe_{2-3}N/Fe_4N$ and porosity
171 plus Fe_4N iron nitride at grain boundaries between 25 and 80 microns below the treated
172 surface. At subsequent depths, polycrystalline cementite of 100-200 nm radius grains is
173 found at grain boundaries nearly parallel to the surface (Figure 2). The case is also
174 characterized by nanometer-scaled nitrides demonstrating the CrN crystallographic
175 structure. No initial carbides (M_7C_3, M = Cr or Fe) from previous tempering or annealing
176 treatments are observed until the depth corresponding to the nitrogen drop-off [7].
177
178 3.2. ASAXS characterization
179

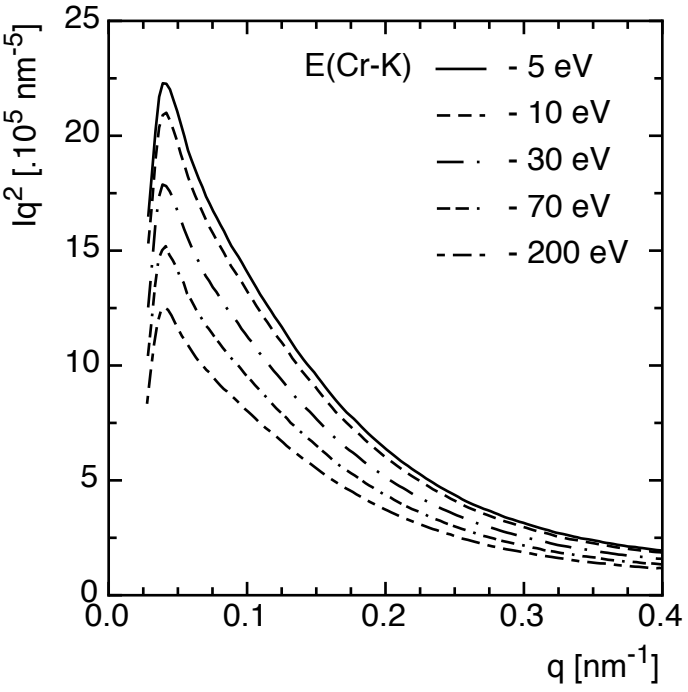

180 (a)

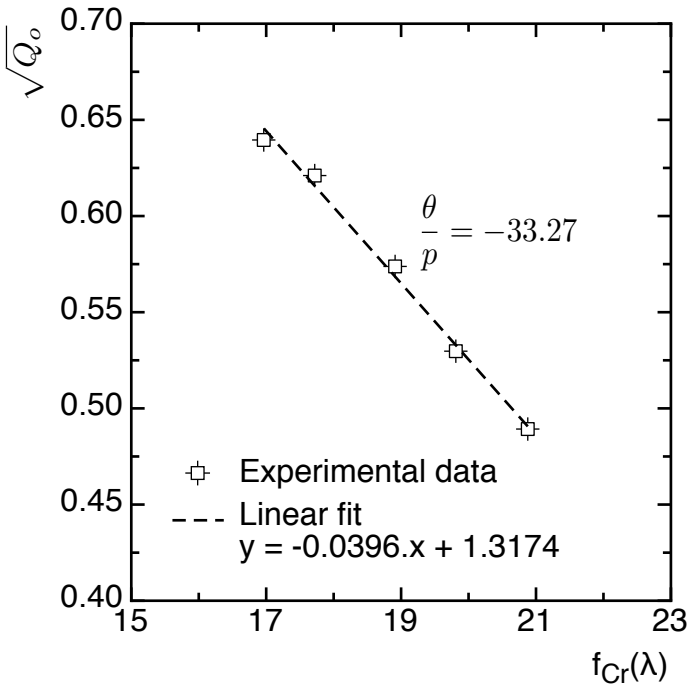

(b)

Figure 3: Sample nitrided at 550 °C for 100 h at a depth z = 400 µm. (a) Evolution of the scattering signal for the various energies used for anomalous SAXS. (b) Plot of $\sqrt{Q_0}$ *vs.* $f_{Cr}(\lambda)$ exhibiting a linear behavior leading to the determination of the θ/p value.

ASAXS measurements were carried out through the nitrided depth, in particular in the diffusion layer. Regarding the size of cementite grains (radius of 100-200 nm) compared to MN nitrides (less than 50 nm), ASAXS conditions were chosen to characterise precipitates in the 2-50 nm radius range. As a consequence, no influence of carbides is expected within the diffusion layer.

Resulting scattering curves are displayed in Figure 3.a in the Iq^2 *vs.* q plot. It is worth noting that only one peak can be observed in this plot, corresponding to only one family of scattering precipitates. This is not surprising since platelets are reported to have comparable diameter (~10-20nm) than globular precipitates, mainly differing by their thickness (~5nm for globular nitrides, and 2nm for platelets) [9], both sizes being investigated in the used q-range. As a consequence, different families of nitrides

(incoherent globular MN formed by transformation carbides and semi-coherent platelets homogeneously nucleated in the matrix) cannot be distinguished. In the following, ASAXS data interpretation will then be conducted irrespectively of the type of nitrides. It is however important to notice that literature reports that both have the same crystal structure and are of MN-type structure [9]. However the composition may vary between both, semi-coherent are expected to be pure CrN precipitates (as in binary Fe-Cr system) whereas nitrides originated from transformed carbides may contain Fe and C in substitution of Cr and N respectively, at least as a transition state. Substituted carbon in MN has little effect on ASAXS experiments regarding that C has only one less electron than N, resulting in similar scattering factors (7.05 and 6.04 e.atom^{-1} for N and C respectively at 5.96 keV). On the contrary, Fe may alter significantly the electronic contrast between nitrides and the matrix. In the following, stoichiometric MN (M=Cr or Fe) nitrides will then be considered as the composition of scattering precipitates.

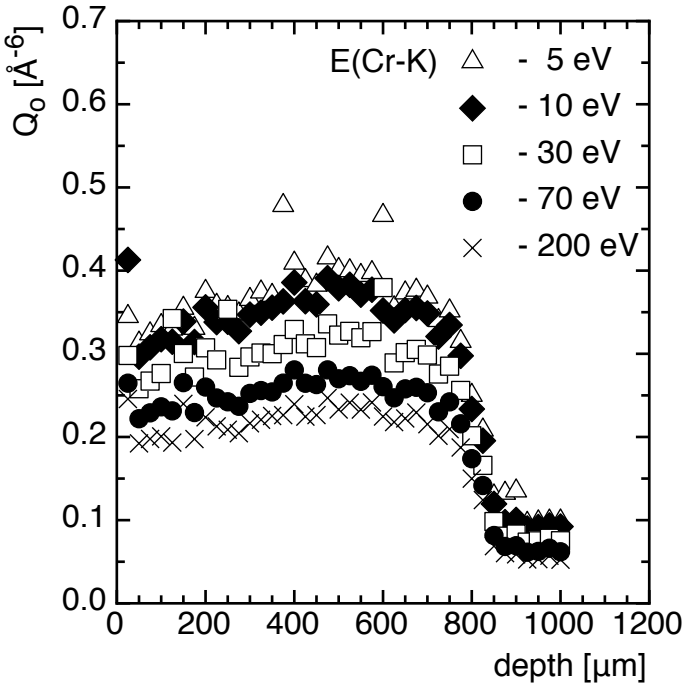

(a)

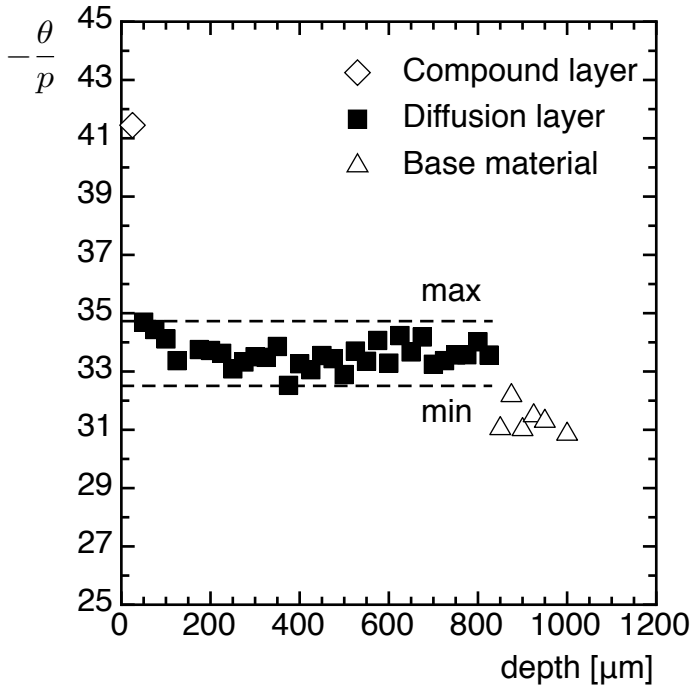

(b)

Figure 4: Sample nitrided at 550 °C for 100 h. (a) Evolution of the integrated intensity for the various energies used for anomalous SAXS with depth (z = 0 corresponds to the surface). (b) Evolution of the -θ/p ratio in the different zones of the nitrided layer.

Regarding the anomalous behaviour, as expected from the increase in the electronic contrast between the nitride and the matrix $\Delta\rho(\lambda)$by approaching the K-edge of Cr, the scattering signal and hence the integrated intensity Q_0 are monotonically varying with the energy. The data treatment detailed in 2.3. is applied to determine the composition of MN nitrides. The linear behaviour of $\sqrt{Q_0}$ with $f_{Cr}(\lambda)$ is displayed in Figure 3.b. Such measuremnts were performed along the nitrided layer and results are displayed in Figure 4. The various regions of the nitrided layer can be easily distinguished. The depth of the diffusion layer is well reproduced and is in agreement with C/N profiles (Figure 1) and with previous studies on this material [7]. The procedure of preparing the ASAXS sample from a bevel through the nitrided sample in order to perfom in-depth scanning of the nitrided layer is as a consequence proven. It can be observed on Figure 4 that the

integrated intensity Q_0 as well as the θ/p ratio are fairly constant in the diffusion layer, more precisely in the 200-700 µm range in depth. This means that the composition (θ/p constant) and the volume fraction (Q_0 and composition constant) of nitrides are almost homogeneous throughout the nitrided layer (apart from boundaries). In the 0-200 µm range in depth, larger nitrides were observed leading to a truncated scattering signal in the small q-range ($q < 0{,}03\ nm^{-1}$); as a consequence the integrated intensity Q_0 is underestimated in this region, leading to underestimated volume fraction of nitrides in the following.

As mentioned previously, data treatment is carried out by considering that scattering precipitates are mainly MN nitrides (M=Cr or Fe). It follows that equation (5) can be written as :

$$\frac{\theta}{p} = \frac{\alpha\left(0.5 f_N + f_{Fe}\left(0.5 - X_{Cr,ppt}\right)\right) - f_{Fe}}{\alpha X_{Cr,ppt}} \qquad \text{equation (8)}$$

considering that $X_{N,ppt} = 0.5$ and that the matrix is defined as pure Fe.

The evolution of the θ/p ratio as a function of $X_{Cr,ppt}$ is plotted on Figure 5. This leads to the determination of the Cr contribution in the chemical composition of MN nitrides and also to the Fe contribution. By considering the whole range of experimental θ/p values, the resulting composition of MN nitrides can be estimated: $Cr_{0,6\pm10\%}Fe_{0,4\pm10\%}N$. The variation of the composition along the depth of the diffusion layer is displayed on Figure 6. The composition is almost constant for depth between 100 µm and 800 µm, corresponding to the diffusion layer.

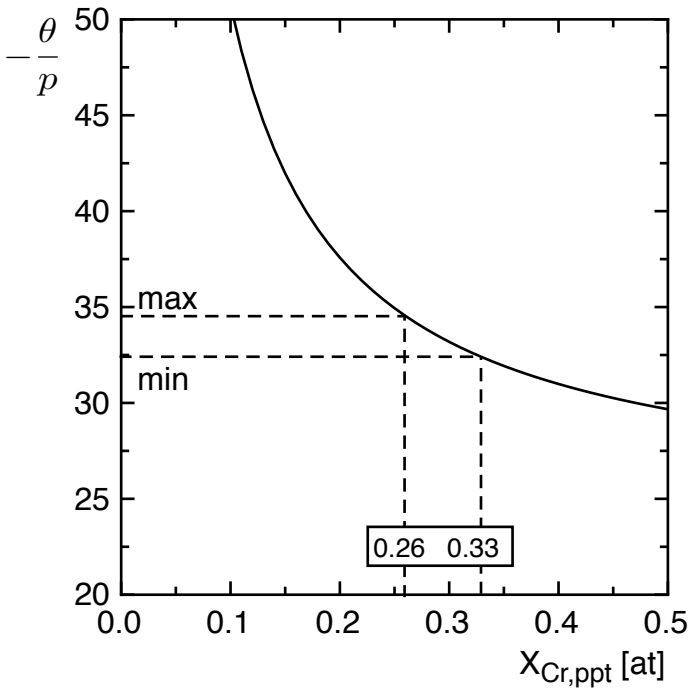

Figure 5: Calculation of the $-\theta/p$ ratio evolution as a function of Cr content in the precipitates $X_{Cr,ppt}$ (in atomic fraction) in the case of MN (M = Fe or Cr, $X_{N,ppt}$ = 0,5) nitrides. min and max correspond to the experimental minimum and maximum values of the $-\theta/p$ ratio as referred in Figure 4.

Once composition of the nitrides determined, the measured Q_0 values can be used to calculate the volume fraction of nitrides formed in the diffusion layer by using equation (1). The evolution of the volume fraction of nitrides as a function of depth is displayed in Figure 7.

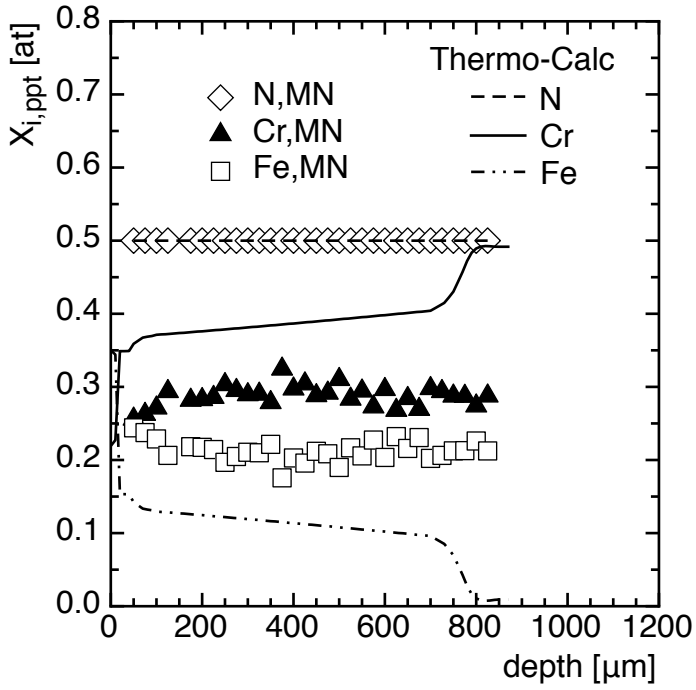

Figure 6: Evolution of the nitride composition as a function of depth (z = 0 corresponds to the surface)

3.3. Thermo-Calc calculations

The Thermo-Calc software (version 4.0 [12] and TC-API version 7.0 [15]) was used to estimate the volume fraction of phases through the case from experimental N/C profiles (Figure 7). It is based on the CALPHAD method and the lattice solubility concept [16]. Calculations were performed at the nitriding temperature and using the Thermo-Calc Software TCFE7 Steels/Fe-alloys database version 7 [17]. According to experimental investigations, some phases were rejected from thermodynamics calculations such as M_6C or M_5C_2 carbides and N_2 gas was not taken into account. Thermodynamics calculations were performed by allowing the presence of iron atoms into MN nitrides such as M = Cr and/or Fe. On one hand, when allowing precipitation of iron into MN nitrides, the atomic

fraction of iron in nitrides (Figure 6) and volume fraction of nitrides (figure 7) are found close to 12 at.% and 6 vol.% respectively along the nitrided depth.

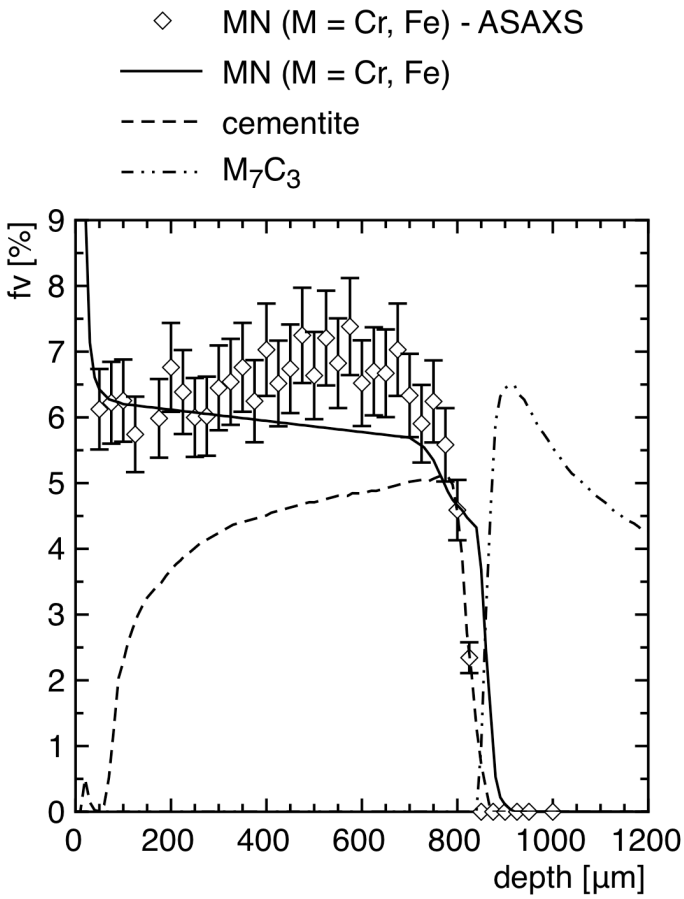

Figure 7: Evolution of the volume fraction of phases through the case after nitriding during 100 h at 550 °C a Fe-0.354wt.%C-2.93wt.%Cr ternary alloy. Comparisons between ASAXS experiments and Thermo-Calc calculations from experimental N and C depth profiles (Figure 1).

3.4. Discussion

The fraction of iron, up to 20 at.% (Figure 6), estimated from ASAXS measurements, and the volume fraction of nitrides (Figure 7) are consistent with thermodynamics calculations performed with the Thermo-Calc software (Figure 7) and with experimental data in the literature [18-20]. Based on matter balance, the fraction of chromium and nitrogen taking part into the precipitation of nitrides was also determined and compared

to the overall element contents. Given the low solubilities of chromium and nitrogen have low solubilities in ferrite (~1.10^{-4} wt.%Cr and 0,05 wt.%N at 550°C), matter balance (Figure 8) gives composition close to the overall content of these elements, supporting the used assumptions.

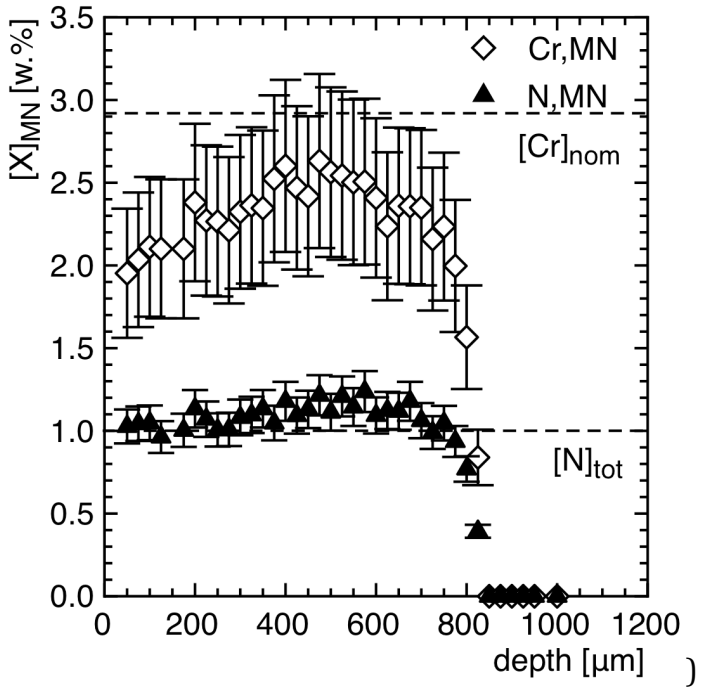

Figure 8: Amount of N and Cr involved in MN nitrides as a function of depth. For comparison, the mean total amount of N, $[N]_{tot}$, as measured by GDOES/EPMA is indicated as well as the nominal Cr composition $[Cr]_{nom}$.

4. Conclusion

ASAXS measurements are used to determine the volume fraction of chromium nitrides on a gas nitrided Fe-0.354wt.%C-2.93wt.%Cr ternary alloy. Although complementary investigation is needed to distinguish different kinds of nitrides, the current study has proven the potentiality of ASAXS technique to provide quantitative data concerning precipitates through thickness in the nitrided layer of Fe-Cr-C steels. Such data are key

parameters for the evaluation of induced volume change and resulting mechanical properties in nitride steels.

Acknowledgements

The authors would like to thank the European Synchrotron Radiation Facilities for giving access to the French CRG beamline BM02-D2AM (Experiment 02-01805) as well as Dr. Martiane CABIE for TEM observations at CP2M, Aix-Marseille University, France. We also thank Aubert & Duval, ERAMET Group, for supplying nitrided steels.

References

[1] G. Goerigk, H.G. Haubold, O. Lyon, J.P. Simon, Anomalous small-angle X-ray scattering in materials science, J Appl Cryst 36 (2003) pp. 425-429

[2] Y. Waseda, Anomalous X-Ray Scattering for Materials Characterization, STMP 179, Springer-Verlag Berlin Heidelberg (2002) pp.161-179

[3] American Society for Metals, Source Book on Nitriding, Metals Park, Ohio : A.S.M. (1977)

[4] E.J. Mittemeijer, Case-Hardened Steels : Microstructural and Residual Stress Effects, edited by D.E. Diesburg, Warrendale, Pennsylvania : TMS-AIME (1984) pp.61

[5] E.J. Mittemeijer, Fundamentals of Nitriding and Nitrocarburizing, ASM Handbook, Volume 4A, Steel Heat Treating Fundamentals and Processes, J. Dossett and G.E. Totten, editors, 2013

[6] K.H. Jack, Nitriding, Proc. Heat Treatment '73, The Metal Society, London, pp. 39-50

[7] S. Jegou, L. Barrallier, R. Kubler, Phase transformations and induced volume changes in a nitrided ternary Fe-3%Cr-0.345%C alloy, Acta Materialia 58 (2010) pp.2666-2676

[8] C. Leroy, H. Michel, M. Gantois, Transformation of $(Cr,M)_7C_3$-type carbides during nitriding of chromium alloyed steels, Journal of Materials Science 21 (1986) pp.3467-3474

[9] J-N. Locquet, R. Soto, L. Barrallier, A. Charaï, Complete investigation of a nitrided

layer for Cr alloy steel, Microscopy Microanalysis Microstructures 8 (1997) pp.335-352

[10] S. Mridha, D. H. Jack, Characterization of nitrided 3% chromium steel, Metal Science 16.8 (1982) pp. 398-404

[11] M. Dumont, L. Commin, I. Morfin, F. De Geuser, F. Legendre, P. Maugis, Chemical composition of nano-phases studied by anomalous small-angle X-ray scattering : Application to oxide nano-particle in ODS steels, Materials Characterization 87 (2014) pp.138-142

[12] J.O. Andersson, T. Helander, L. Höglund, P.F. Shi, and B. Sundman, Thermo-Calc and DICTRA, Computational tools for materials science, Calphad 26 (2002) pp.273-312

[13] P.C. Van Wiggen, H.C.F. Rozendaal, E.J. Mittemeijer, The nitriding behaviour of iron-chromium-carbon alloys, Journal of Materials Science 20 (1985) pp.4561-4582

[14] S. Jegou, L. Barrallier, R. Kubler, M.A.J. Somers, Evolution of residual stress in the diffusion zone of a model Fe-Cr-C alloy during nitriding, HTM J. Heat Treatm. Mat. 66(3) (2011) pp.135-142

[15] Thermo-Calc Software TC-API User's Guide version 7.0, (Accessed 19 June 2014)

[16] L. Kaufman, H. Bernstein, Computer Calculation of Phase Diagrams, Academic Press, New-York (1970)

[17] Thermo-Calc Software TCFE7 Steels/Fe-alloys database version 7.0, (Accessed 23 Aug 2013)

[18] R. Danoix, L. Legras, B. Hannoyer, J. Dulcy, F. Danoix, Solid to Solid Transformations in Inorganic Materials (PTM) 2005, Edited by J.M. Howe, D.E. Laughlin, J.K. Lee, U. Dahmen and W.A. Soffa, TMS (The Minerals, Metals and Material Society) 2005, Vol. 1 : Diffusional Transformations, pp. 351-356

[19] C. Ginter, L. Torchane, J. Dulcy, M. Gantois, A. Malchere, C. Esnouf, T. Turpin, A new approach to hardening mechanisms in the diffusion layer of gas nitrided α-alloyed steels. Effects of chromium and aluminium : experimental and simulation studies, La Metallurgia Italiana 7-8 (2006) pp. 29-35

[20] P. Jessner, R. Danoix, B. Hannoyer, F. Danoix, Investigations of the nitrided subsurface layers of an Fe-Cr model alloy, Ultramicroscopy 109 (2009) pp. 530-534